UNIVERSITY OF LIVERPOOL

Modelling Competing Bacterial Species

MATH554

Alexander Totir

201178215

2020

Contents

1 Summary

Since reaction-diffusion equations can describe the distribution of concentration, mathematical models based on these equations can be developed with a wide range of application. In population dynamics, the density and spread of a species can be described by reaction-diffusion equations, in which the reaction term refers to their reproduction, while the diffusive term describes the motion of individuals. From these equations, travelling wave solutions can be derived to provide a clearer understanding of the dynamics of a system. Physical applications of these methods include improving our understanding of the movement of bacterial populations around the body, or the growth and spread of tumours.

The aim of this paper is to accurately model competing bacterial species, subject to varying parameters and conditions. The use of travelling wave solutions as methods of solving parabolic equations is explored, with focus on solving and modelling the Lotka-Volterra competition model. The Fisher and Fitzhugh equations will first be detailed to provide a base understanding of how to generate travelling wavefront solutions and how minimum wavespeed requirements are derived. Analytic analysis of the Lotka-Volterra model then uses the systems' Jacobian matrix to determine the steady states and resultant eigenvalues at each point, in turn providing the wavespeed requirements of transitions involving each state. The explicit finite forward difference method is then implemented to understand the numerical method used in the later simulations, as well as the conditions necessary for stability. Finally, numerical simulations are ran to explore the behaviour of the system for different cases, along with understanding the results of wavefront transitions between different steady states.

2 Statement of Originality

This dissertation was written by me, in my own words, except for quotations from published and unpublished sources which are clearly indicated and acknowledged as such. I am conscious that the incorporation of material from other works or a paraphrase of such material without acknowledgement will be treated as plagiarism, according to the University Academic Integrity Policy. The source of any picture, map or other illustration is also indicated, as is the source, published or unpublished, of any material not resulting from my own research.

3 Introduction

In this section, the theory of travelling waves will be explored, with particular focus on their use as solutions to nonlinear partial differential equations. Moving on, reaction-diffusion systems will be detailed before turning the focus to the use of travelling waves as solutions to such systems, followed by solving two example reaction-diffusion equations: the Fisher equation and the Fitzhugh equation.

3.1 Travelling Waves

A travelling wave is a wave that moves in a particular direction, propagating with a constant speed c. While there exist several different forms of travelling waves, this paper will particularly focus on travelling wavefronts, waves that move through space from one constant state to another without oscillation. Due to being functions of space and time, travelling waves are fundamental in many mathematical equations with applications in a wide range of fields, with their use most fully developed for solving partial differential equations [10]. Using travelling wave solutions for a system of PDEs allows us to model and understand the dynamics of that system.

Travelling wave solutions are expressed as:

$$u(x,t) = U(z), \quad z = x - ct \tag{1}$$

where c represents the speed of the propagating wave and x and t represent the spatial and time domains respectively. In the case of $c = 0$ the wave is classed as stationary, meaning it does not propagate. For a travelling wave solution to be classed as a travelling wavefront, we require

$$U(-\infty) = u_{left}, \quad U(\infty) = u_{right}, \quad u_{left} \neq u_{right} \tag{2}$$

meaning the wave travels from one steady state at $U(-\infty)$ to another steady state at $U(\infty)$.

3.2 Reaction-Diffusion Systems

Reaction-diffusion equations describe the change in space and time of the concentration of one or more substances. As the name suggests, such equations are comprised of a reaction term and a diffusion term and arise in systems involving interacting components, with a use in mathematical biology when modelling interacting populations.

The simplest case of the nonlinear reaction-diffusion equation is

$$\frac{\partial u}{\partial t} = R(u) + D\frac{\partial^2 u}{\partial x^2}, \tag{3}$$

which is a partial differential equation representing a reaction-diffusion system in one spatial dimension. The $D\frac{\partial^2 u}{\partial x^2}$ term describes the diffusion, in which D represents the diffusion coefficient. The $R(u)$ term represents a function that describes a change in parameter u.

3.2.1 Fisher Equation

In 1937, Fisher suggested the equation

$$\frac{\partial u}{\partial t} = ku(1-u) + D\frac{\partial^2 u}{\partial x^2} \tag{4}$$

to describe the spatial spread of a favoured allele in a population [8], however it can also be applied to the spread of any biological population. The terms $ku(1-u)$ and $D\frac{\partial^2 u}{\partial x^2}$ are the reaction and diffusion terms respectively, while D represents the diagonal matrix of diffusion coefficients. This equation is the natural extension of the logistic growth model, to incorporate the diffusion of a population in space.

To solve equation (4) and test for the existence of a travelling wavefront solution, we must first nondimensionalise the equation by writing:

$$t^* = kt, \quad x^* = x\left(\frac{k}{D}\right)^{\frac{1}{2}}$$

Rewriting as

$$t = \frac{t^*}{k}, \quad x = x^*\left(\frac{D}{k}\right)^{\frac{1}{2}},$$

we can substitute these into equation (4) to give

$$\frac{\partial u}{\partial\left(\frac{t^*}{k}\right)} = ku(1-u) + D\frac{\partial^2 u}{\partial\left(\frac{(x^*)^2 D}{k}\right)}$$

After bringing the constants out of the derivatives and cancelling down k and D, along with omitting the asterisks for notational simplicity, equation (4) reduces down to

$$\frac{\partial u}{\partial t} = u(1-u) + \frac{\partial^2 u}{\partial x^2} \tag{5}$$

For the spatially homogeneous problem, when $\frac{\partial^2 u}{\partial x^2} = 0$, there exist two steady states at $u = 0$ and $u = 1$, which are unstable and stable respectively. Combining this with the fact $u < 0$ is not physically possible, we must look for a travelling wavefront solution in the region $0 \leq u \leq 1$. Such a solution will take the form seen in (1). However, the invariance of equation (5) if $x \to -x$ means c can be positive or negative, so for simplicity we will use

$c \geq 0$. Substituting this form of travelling wave $U(x - ct)$ into equation (5), U(z) satisfies

$$U'' + cU' + U(1 - U) = 0 \tag{6}$$

As described in (2), a typical wavefront solution involves U at one end being at a different steady state than at the other end. Therefore, we seek a solution for which

$$\lim_{z \to +\infty} U(z) = 0, \quad \lim_{z \to -\infty} U(z) = 1. \tag{7}$$

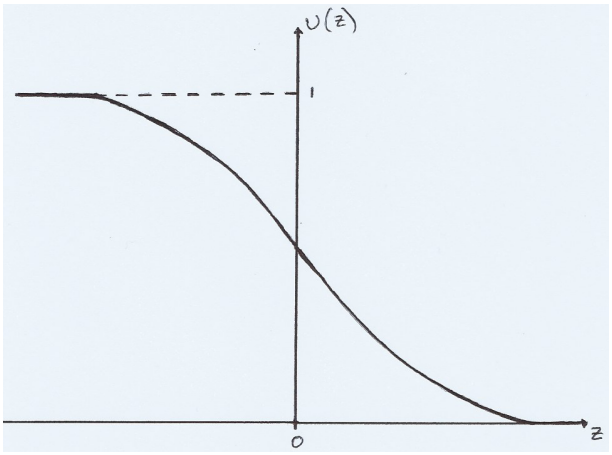

Figure 1: **Travelling wavefront diagram.** A simple travelling wavefront, moving from $U(-\infty) = 1 \to U(\infty) = 0$.

To do this, we must transform (6) into two separate first order ODEs. These are:

$$U' = V, \quad V' = -cV - U(1 - U) \tag{8}$$

From these, we can calculate the phase plane trajectories as solutions of

$$\frac{dV}{dU} = \frac{-cV - U(1 - U)}{V}, \tag{9}$$

with this equation containing two stationary points in the (U, V) plane: $(0, 0)$ and $(1, 0)$. For stability analysis, we must first linearise the equation around each of these points by writing

$$U = U^* + dU, \quad V = V^* + dV \tag{10}$$

where dU, dV represent the change in U and V respectively and the asterisk indicates the fixed point around which the equation is being linearised. Next, we form the Jacobian matrix

$$\frac{d}{dt}\begin{bmatrix} dU \\ dV \end{bmatrix} = \begin{bmatrix} \frac{df}{dU} & \frac{df}{dV} \\ \frac{dg}{dU} & \frac{dg}{dV} \end{bmatrix}\Bigg|_* \begin{bmatrix} dU \\ dV \end{bmatrix} \tag{11}$$

where $f = U' = V$ and $g = V' = -cV - U(1-U)$. Therefore, we have

$$\frac{d}{dt}\begin{bmatrix} dU \\ dV \end{bmatrix} = \begin{bmatrix} 0 & 1 \\ -1+2U & -c \end{bmatrix}\Bigg|_* \begin{bmatrix} dU \\ dV \end{bmatrix} \tag{12}$$

At $(0,0)$, this matrix reduces to

$$\begin{bmatrix} 0 & 1 \\ -1 & -c \end{bmatrix}$$

which contains the eigenvalues

$$\lambda_\pm = \frac{-c \pm \sqrt{c^2-4}}{2} \Rightarrow \begin{cases} \text{stable node} & \text{if } c^2 \geq 4 \\ \text{stable spiral} & \text{if } c^2 \leq 4 \end{cases}$$

At $(1,0)$, we have

$$\begin{bmatrix} 0 & 1 \\ 1 & -c \end{bmatrix}$$

which produces the eigenvalues

$$\lambda_\pm = \frac{-c \pm \sqrt{c^2+4}}{2} \Rightarrow \text{ saddle point}$$

From this analysis, we can see that if $c \geq c_{\min} = 2$, the origin is a stable node. If $c^2 < 4$ then the origin is a stable spiral, meaning U oscillates around this point. However, while travelling wave solutions exist for $c < 2$, they do not represent real solutions since $U < 0$ denotes a negative population, which is a physical impossibility. This is shown with the spiralling of the trajectories around the origin, meaning they enter the negative quadrants at certain points.

This analysis highlights that for a real travelling wave solution to exist, all wavespeeds must satisfy $c \geq c_{\min} = 2$. For our initial dimensional equation (4), all wavespeeds must satisfy

$$c \geq c_{\min} = 2\sqrt{kD} \tag{13}$$

However, the resultant wavespeed is also defined by the shape of the wave profiles. For example, if the wave profile has the form $e^{-\alpha Z}$, changes in α will change the shape of the profile and therefore affect the wavespeed. In this scenario, the wavespeed will decay rather than be given by a step function. The wavespeed can be any value, provided it is higher than the

minimum requirement. The shape of the wave profile can also be affected by changing the initial conditions of the system.

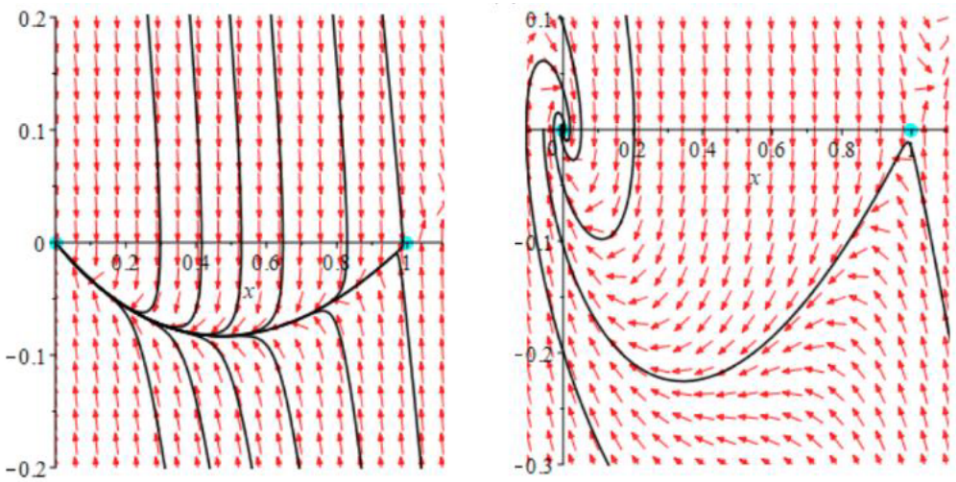

Figure 2: **Phase plane trajectories for equation (6)**. On the left, for $c > c_{min} = 2$, the point $(0, 0)$ is a stable node. On the right, for $c^2 < 4$, the point $(0, 0)$ is a stable spiral, with the trajectories oscillating around the origin. In both cases, the point $(1, 0)$ is a saddle node. Taken from [**?**].

3.2.2 Fitzhugh Equation

Another example of a reaction-diffusion equation is the excitable kinetics model represented by the Fitzhugh equation. This biological mechanism models a biochemical 'switch', where a large peturbation of Ca^{2+} (calcium) ions moves the system from one steady state to another [7]. The reaction diffusion equation for this model is:

$$\frac{\partial u}{\partial t} = A(u - u_1)(u_2 - u)(u - u_3) + D\frac{\partial^2 u}{\partial x^2} \tag{14}$$

which represents a cubic parabola, in contrast to the square parabolic Fisher equation. Here, A is a positive constant representing the autocatalytic release of calcium ions, u represents the concentration of calcium with $u_1 < u_2 < u_3$, while again D is the diffusion coefficient. The terms u_1, u_2, u_3 represent the respective steady states, with u_1, u_3 stable and u_2 unstable. We must now assume there exist wavefront solutions for equation (14), which must be of the form

$$u(x, t) = U(z), \quad z = x - ct \tag{15}$$

for which

$$\lim_{z \to +\infty} U(z) = u_1, \quad \lim_{z \to -\infty} U(z) = u_3 \tag{16}$$

Substituting this form of solution into (14) gives

$$DU'' + cU' + A(U - u_1)(u_2 - U)(U - u_3) = 0 \tag{17}$$

Again, we seek solutions of a simpler differential equation that U satisfies. Therefore, we try to make U satisfy the first order differential equation:

$$U' = a(U - u_1)(U - u_3) \tag{18}$$

Substituting this into equation (17), we obtain:

$$(U - u_1)(U - u_3)Da^2(2U - u_1 - u_3) + ca - A(U - u_2) = 0 \tag{19}$$

which can be rewritten as

$$(U - u_1)(U - u_3)[U(2Da^2 - A) - [Da^2(u_1 + u_3) - ca - Au_2]] = 0 \tag{20}$$

For this to be true, we require:

$$2Da^2 - A = 0, \quad Da^2(u_1 + u_3) - ca - Au_2 = 0$$

From this, we can determine a and c as:

$$a = \left(\frac{A}{2D}\right)^{\frac{1}{2}}, \quad c = \left(\frac{AD}{2}\right)^{\frac{1}{2}}(u_1 - 2u_2 + u_3) \tag{21}$$

Unlike the Fisher equation, the calculated wavespeed c of this equation is unique.

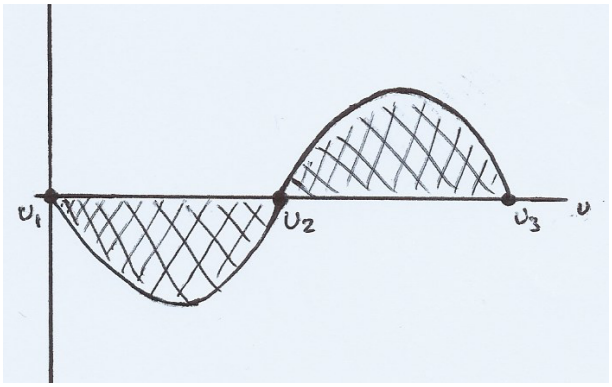

Figure 3: **Stationary bistable cubic parabola diagram.** u_1, u_3 are stable, u_2 is unstable. Here, u_2 is centred between u_1 and u_3, meaning the wave is stationary.

Equation (14) can also be represented by a cubic parabola, which allows us to calculate the wave velocity as a ratio of a constant multiplied by an

integral, with the integral term representing the area between the curve and the horizontal axis. The total area under the parabola gives indication of the direction in which the wavefront is travelling. From the wavespeed c calculation in equation (21), we can see that if u_2 is exactly half way between u_1 and u_3, then we have

$$c = \left(u_1 - 2 \left(\frac{u_3 + u_1}{2} \right) + u_3 \right) = 0$$

hence we have a stationary wave, as shown in figure 3. For values of u_2 closer to u_1 than to u_3, the overall area under the parabola becomes positive, meaning the wave moves along the x axis in the positive direction. If u_2 is closer to u_3, the total area is negative meaning the wave moves horizontally in the negative direction.

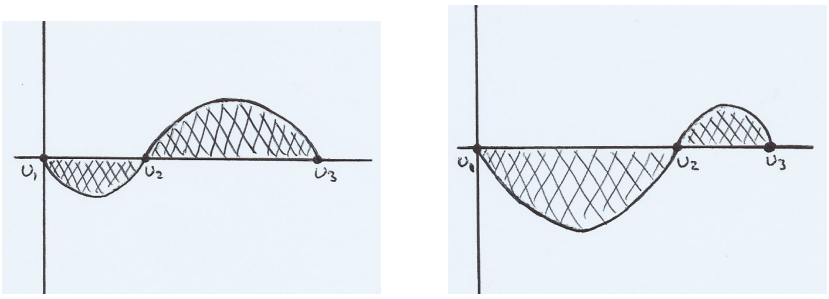

(a) Positive Area (b) Negative Area

Figure 4: **Travelling bistable cubic parabola diagrams.** u_1, u_3 are stable, u_2 is unstable. (a) and (b) show how the variance of u_2 affects the total area under the parabola. (a) involves a wavefront travelling right due to the total positive area, while (b) indicates a wavefront travelling left.

Another method to solve equation (17) is to take the generalised equation:

$$U'' + cU' + F(U) = 0 \tag{22}$$

with the aforementioned conditions

$$\lim_{z \to +\infty} U(z) = u_1, \quad \lim_{z \to -\infty} U(z) = u_3 \tag{23}$$

and regard equation (22) as a sum of three terms that total zero, with the primes denoting derivatives over z. This equation can be multiplied by U' and integrated over z, from $-\infty$ to ∞, giving us:

$$\int_{-\infty}^{\infty} U''U'dz + c\int_{-\infty}^{\infty} U'^2 dz + \int_{-\infty}^{\infty} F(U)U'dz = 0 \tag{24}$$

Integrating the first term gives $\frac{U'^2}{2}$, meaning this integral term is zero due to its saturation at $\pm\infty$. The second terms involves the wavespeed c multipled by an unknown term $\int_{-\infty}^{\infty} U'^2 dz$. However, since the integral is of a squared number, we can conclude the unknown term is greater than zero. The final term $\int_{-\infty}^{\infty} F(U)U'dz$ can be reduced down since

$$U' = \frac{dU}{dz} \Rightarrow \frac{dU}{dz}dz = dU$$

therefore, we have

$$\int_{-\infty}^{\infty} F(U)dU$$

Since we know that at $-\infty$, $U = u_3$ and at ∞, $U = u_1$, this term reduces down to the integral from u_3 to u_1, which represents the shaded area under the parabola seen in figures 3 and 4. We now have

$$c = -\frac{\int_{-\infty}^{\infty} F(U)dU}{\int_{-\infty}^{\infty} U'^2 dz}$$

and since we know the denominator term is strictly positive, we can see that the resultant wavespeed c is dependent on whether the area under the parabola seen in figures 3 and 4 is positive or negative.

4 Analytic Study of Lotka-Volterra Competition Model

We can expand on the spatially homogeneous Lotka-Volterra competition model to incorporate the diffusive terms of the respective species, M and N. This creates the system:

$$\begin{cases} M_t = D_1 M_{xx} + r_1 M \left[1 - \frac{M}{K_1} - a_1 \frac{N}{K_1}\right] \\ N_t = D_2 N_{xx} + r_2 N \left[1 - \frac{N}{K_2} - a_2 \frac{M}{K_2}\right] \end{cases} \tag{25}$$

where $D_1, D_2, r_1, r_2, K_1, K_2, a_1$ and a_2 are all positive constants. D_1 and D_2 represent the respective diffusion coefficient of each population, r_1 and r_2 represent the linear birth rates of each species and the K terms represent the maximum carrying capacity of each population. The a_1 and a_2 terms measure the competitive effect of N on M and M on N respectively. To solve this system, it must first be nondimensionalised, to give:

$$\begin{cases} u_t = u_{xx} + u(1 - u - b_1 v) \\ v_t = d v_{xx} + \rho v(1 - v - b_2 u) \end{cases} \tag{26}$$

where d is a ratio of the two diffusion coefficients D_1 and D_2 and ρ represents the ratio of proliferation rates r_1 and r_2. The b_1 and b_2 terms now represent the competitive effect of each species, with their values providing an indication to the type of competition that is present. For $b_1, b_2 < 1$ the competition is described as weak. For either $b_1 < 1, b_2 > 1$ or $b_1 > 1, b_2 < 1$, there is weak strong competition between the species. Finally, for $b_1, b_2 > 1$, strong competition is occurring.

Currently however, system (26) will have infinitely many solutions, meaning it requires initial conditions and boundary conditions to be complete and provide a unique solution. The initial conditions will be specified and subject to change throughout the numerical calculations. In contrast, the boundary conditions remain constant throughout. Neumann boundary conditions are being used, meaning the normal derivatives of each dependent variable are specified at the boundary. To help implement this type of boundary condition, we introduce the ghost points $U(1)$ and $U(n)$ next to the boundary. In the MATLAB code, we specify $U(1) = U(2)$ and $U(n) = U(n-1)$, so that the boundaries $U(1)$ and $U(n)$ are never touched. The boundary conditions can also be described as zero flux, since the gradients between the points $U(1)$ and $U(2)$, as well as between $U(n)$ and $U(n-1)$, are zero.

Using the form of travelling wave solution $u(x,t) = U(x - ct)$, system 26 satisfies

$$\begin{cases} cU' = U'' + u(1-u-b_1v) \\ cV' = dv'' + \rho v(1-v-b_2u) \end{cases} \tag{27}$$

To find the wavefront solution, we must first transform this system into four first order ODEs:

$$\begin{cases} \frac{\partial u}{\partial \mathcal{E}} = w, \frac{\partial w}{\partial \mathcal{E}} = cw - u(1-u-b_1v) \\ \frac{\partial v}{\partial \mathcal{E}} = s, \frac{\partial s}{\partial \mathcal{E}} = \frac{cs-\rho v(1-v-b_2u)}{d} \end{cases} \tag{28}$$

Using these equations, we can construct the systems' 4x4 Jacobian matrix from which the equilibrium points and their respective eigenvalues can be calculated. This can be done using MATLAB to produce the following matrix of equilibria:

$$\begin{bmatrix} 0 & 0 & 0 & 0 \\ 1 & 0 & 0 & 0 \\ 0 & 0 & 1 & 0 \\ \frac{b_1-1}{b_1b_2-1} & 0 & \frac{b_2-1}{b_1b_2-1} & 0 \end{bmatrix} \tag{29}$$

with the columns representing the partial derivatives of each equation with respect to $[u, w, v, s]$. As expected, the same four as in the spatially homogeneous case are present, but with zeroes for the variables w and s. These are: the extinction state $(0, 0)$, two monoculture states $(0, 1)$ and $(1, 0)$ and the coexistence state $(\frac{b_1-1}{b_1b_2-1}, \frac{b_2-1}{b_1b_2-1})$.

Due to the coexistence equilibrium not being constrained to obvious parameters, along with the eigenvalues for this state being simply too long to be included, we only have interest in the points $(0, 0), (1, 0)$ and $(0, 1)$. The eigenvalues for these states are calculated as:

$$e_1 = \begin{cases} \frac{c}{2} - \frac{\sqrt{(c-2)(c+2)}}{2} \\ \frac{c}{2} + \frac{\sqrt{(c-2)(c+2)}}{2} \\ \frac{c+\sqrt{c^2-4d\rho}}{2d} \\ \frac{c-\sqrt{c^2-4d\rho}}{2d} \end{cases} \tag{30}$$

$$e_2 = \begin{cases} \frac{c}{2} - \frac{\sqrt{c^2+4}}{2} \\ \frac{c}{2} + \frac{\sqrt{c^2+4}}{2} \\ \frac{c+\sqrt{c^2-4d\rho+4b_2d\rho}}{2d} \\ \frac{c-\sqrt{c^2-4d\rho+4b_2d\rho}}{2d} \end{cases} \tag{31}$$

$$e_3 = \begin{cases} \frac{c}{2} - \frac{\sqrt{c^2+4b_1-4}}{2} \\ \frac{c}{2} + \frac{\sqrt{c^2+4b_1-4}}{2} \\ \frac{c+\sqrt{c^2+4d\rho}}{2d} \\ \frac{c-\sqrt{c^2+4d\rho}}{2d} \end{cases} \tag{32}$$

where e_1 corresponds to the state $(0, 0)$, e_2 corresponds to $(1, 0)$ and e_3 corresponds to $(0, 1)$.

For travelling wavefront solutions to exist, all eigenvalues for each point must be real. Therefore, we are required to find the minimum value of c that satisfies this condition, in turn providing minimum wavespeed requirements for each state.

For e_1, we have four eigenvalues. $\frac{c}{2} \pm \frac{\sqrt{(c-2)(c+2)}}{2}$ requires

$$c > c_{min} = 2 \tag{33}$$

with $c < 2$ indicating a spiral node. For the eigenvalues $\frac{c+\sqrt{c^2-4d\rho}}{2d}$, we require

$$c > c_{min} = 2\sqrt{d\rho} \tag{34}$$

Since these wavespeed requirements relate to the eigenvalues for the state $(0, 0)$, any travelling wavefront solutions that can be found will involve transitions from this state. However, it can be noted that there is a discrepancy between the two wavespeed requirements, since they are only equal when $d\rho = 1$. This discrepancy will be explored in the numerical results section, where it was found that the wavespeed requirement $c_{min} > 2$ applies only to the wavefronts for species u, while $c_{min} > 2\sqrt{d\rho}$ applies to wavefronts for species v, a fact that was not expected prior to investigation.

For e_2, we require

$$c > c_{min} = 2\sqrt{d\rho(1 - b_2)} \tag{35}$$

This wavespeed requirement stems from the eigenvalues relating to the state $(1, 0)$, meaning any numerical simulations involving transitions from this point will adhere to this wavespeed minimum. This wavespeed requirement can correspond to wave profiles of both species.

For e_3, we require

$$c > c_{min} = 2\sqrt{1 - b_1} \tag{36}$$

Any numerical results following this wavespeed requirement will involve transitions from the state $(0, 1)$. Again, this wavespeed requirement can apply to wavefronts for both species.

The stability for each equilibrium is to be examined, where consideration must also be given to the values of b_1 and b_2. The strict positivity of each eigenvalue for the point $(0, 0)$ indicates that it is an unstable node. For values of $b_1, b_2 < 1$, there exists only one stable point for the system, the coexistence equilibrium. Here, there is a travelling wave $U(x - ct)$ with

$$U(-\infty) = \alpha, \quad U(\infty) = 0$$

indicating the wave transitioning from the steady state $(0, 0)$ to the coexistence point α.

For $b_1 > 1, b_2 < 1$ and $b_1 < 1, b_2 > 1$, the conditions only permit one stable point, $(0, 1)$ and $(1, 0)$ respectively, with the other three equilibrium points for each condition being unstable. Travelling wavefront solutions here will involve transitions from these respective unstable steady states. For $b_1, b_2 > 1$, the system is multistable containing two steady states $(1, 0)$ and $(0, 1)$, with a separatrix splitting the domains of attraction to each point. This means the systems' initial conditions or parameters will determine the resultant equilibrium and travelling wavefronts will transition between these two states.

5 Numerical Scheme

To be able to create computer simulations describing the time evolution of the Lotka-Volterra competition model, the finite-difference method, a type of numerical analysis, is utilised on the partial differential equations to approximate the solutions of the system at progressive time steps. More specifically, the explicit forward difference method is used to determine the solutions. This is a discretisation that solves the differential equations by approximating them with difference equations that finite difference approximates the derivatives [9]. In contrast to implicit numerical methods, which use unknown quantities at the next time step to approximate solutions, explicit methods use known quantities from the previous time step for approximations. Using explicit methods as opposed to implicit makes the future coding simpler, along with reducing the computational power required to generate results.

To do this, the time and space components of the system are uniformly partitioned so that consecutive points of each are separated by Δt and Δx respectively. The partial differential equations are then converted into a system of recurrence equations, by replacing the derivatives in the equations with approximations, that can be solved by matrix algebra techniques. Using u_j^n and v_j^n to denote the approximations of u and v respectively in position j at time n, the method computes each progressive value of u_j^{n+1} and v_j^{n+1} as a function of the respective value at time n. The time derivative $\frac{\partial u}{\partial t}$ is estimated using

$$\frac{\partial u}{\partial t} \approx \frac{u_j^{n+1} - u_j^n}{\Delta t}$$

and the dispersion term is estimated using

$$\frac{\partial^2 u}{\partial x^2} \approx \frac{u_{j+1}^n - 2u_j^n + u_{j-1}^n}{\Delta x^2}$$

The same approximations are also used for population v. These approximations can now be substituted into system (26) to give us the recurrence equations:

$$\begin{cases} \frac{u_j^{n+1} - u_j^n}{\Delta t} = \frac{u_{j+1}^n - 2u_j^n + u_{j-1}^n}{\Delta x^2} + u_j^n(1 - u_j^n - b_1 v_j^n) \\ \frac{v_j^{n+1} - v_j^n}{\Delta t} = d\frac{v_{j+1}^n - 2v_j^n + v_{j-1}^n}{\Delta x^2} + \rho v_j^n(1 - v_j^n - b_2 u_j^n) \end{cases} \tag{37}$$

Solving for u_j^{n+1} and v_j^{n+1}:

$$\begin{cases} u_j^{n+1} = \left(\frac{\Delta t}{\Delta x^2}\right)(u_{j+1}^n - 2u_j^n + u_{j-1}^n) + \Delta t u_j^n(1 - u_j^n - b_1 v_j^n) + u_j^n \\ v_j^{n+1} = d\left(\frac{\Delta t}{\Delta x^2}\right)(v_{j+1}^n - 2v_j^n + v_{j-1}^n) + \Delta t \rho v_j^n(1 - v_j^n - b_2 u_j^n) + v_j^n \end{cases} \tag{38}$$

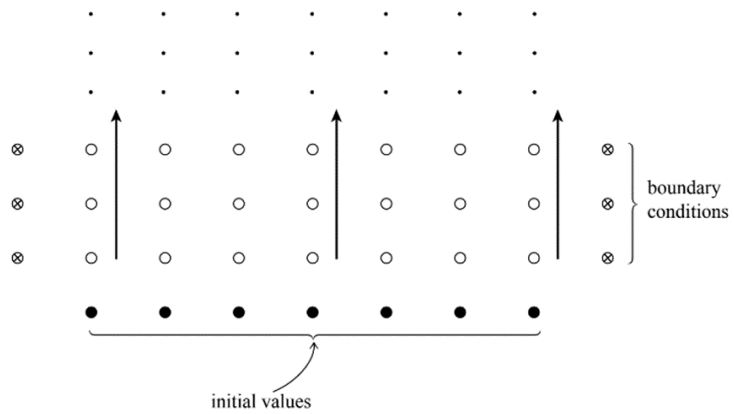

Figure 5: **The initial value problem.** Following the arrows, successive solutions are calculated as the system advances in time. Taken from [9].

Figure 5 provides a visual representation of the finite difference method. The shaded circles denote the initial conditions of the system, which represent the intiation of the wave and will be stated for each case in the numerical section. The hollow circles represent the successive solutions progressing upwards as time advances. On the right and left of the diagram are the Neumann boundary conditions, represented by the crossed circles. As stated in section 4, these are ghost points that lie just outside the domain so that they are never touched. Neumann boundary conditions imply

$$\frac{du}{dx} = 0, \qquad \frac{dv}{dx} = 0 \tag{39}$$

when $x = 0$ or $x = L$, with 0 and L denoting the borders of the medium of size L. Since the derivatives are equal to zero, the boundary has zero flux. This corresponds to physical boundaries and means nothing can pass across the boundary.

Returning to system 38 however, this method is unstable, meaning we must introduce the Neumann stability analysis to provide a more applicable method [9]. This local analysis treats the difference equation coefficients as constant in both space and time, to create independent solutions of the form

$$u_j^n = \xi^n e^{ikj\Delta x} \tag{40}$$

where k represents a real spatial wave number and $\xi = \xi(k)$ is a complex number dependent on k. Since the time dependence of each independent solution is a successive integer power of ξ, the difference equations are unstable for $\xi(k) > 1$ due to the resultant exponential growth. The number ξ provides the amplification factor at a given wave numer k. By substituting 40 into system 37, the amplification factor is found to be

$$\xi = 1 - \frac{4D\Delta t}{(\Delta x)^2} sin^2\left(\frac{k\Delta x}{2}\right) \tag{41}$$

This equation dictates the result of disturbances to the system. As mentioned, $\xi(k) > 1$ causes the system to blow up since it creates exponential growth. For $\xi(k) \leq 1$, the system collapses, leading to the stability criterion requirement of

$$\frac{2D\Delta t}{(\Delta x)^2} \leq 1 \tag{42}$$

Thus, for $D = 1$, the explicit method is convergent and numerically stable for values of

$$\frac{\Delta t}{\Delta x^2} \leq \frac{1}{2}, \tag{43}$$

meaning the MATLAB code must be tailored to achieve a value of $\frac{\Delta t}{\Delta x^2}$ as close to $\frac{1}{2}$ as possible. The calculations are optimised as $\frac{1}{2}$ is approached, leading to a faster algorithm and increasingly accurate results. Therefore, a time step size of $\Delta t = \frac{0.99hx^2}{2d}$ has been selected, so that along with denoting $\Delta x^2 = hx^2$, we get:

$$\frac{\Delta t}{\Delta x^2} = \frac{\frac{0.99hx^2}{2}}{hx^2} = \frac{0.99}{2} < \frac{1}{2}$$

for $d = 1$. This value of $\frac{\Delta t}{\Delta x^2}$ is sufficiently close to $\frac{1}{2}$. Many space step sizes were experimented with, in an attempt to generate results that are as accurate as possible, in the shortest time, since long simulations are time consuming. Therefore, a space step of $hx = 0.1$ was selected since it provided an appropriate balance of duration and accuracy, generating results with an acceptable error margin of 2%.

6 Numerical Simulations

This section includes the MATLAB results produced when calculating the wavespeeds for system (26) with varying parameters and conditions. Using the finite forward difference method, the code plots the wavefronts of u and v at different time steps, to visually represent the different evolutions of the system over time. The code uses a medium of size 100 and a total time of 50. The space is divided up into equal segments to provide the space steps, denoted hx, of size 0.1. The size of the time steps, ht, is given by $\frac{0.99hx^2}{2d}$.

6.1 Transitions from trivial unstable steady state to coexistence

The following figures involve wavefronts transitioning from the unstable steady state $(0, 0)$, where the minimum wavespeed requirement will stem from equation (34), $c_{min} = 2\sqrt{d\rho}$. In the case of $d\rho = 1$, the wavefronts for both species move with the same speed, where $c = 2$.

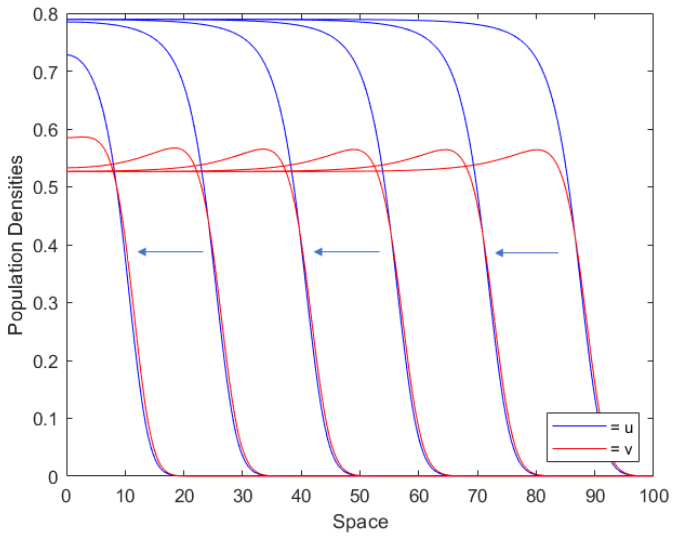

Figure 6: **Wave profiles transitioning from (0,0) to coexistence.** $d = \rho = 1$, $b_1 = 0.4$, $b_2 = 0.6$. The initial conditions $U(0) = 0.3$, $V(0) = 0.5$ are true for the first five grid points, everywhere else they are zeroes. The wavefronts are plotted at times 8, 16, 24, 32, 40 and 48.

Figure 6 shows the evolution of system (26), subject to the specified parameters, in which the wavespeeds are calculated as c=1.9903. As previously mentioned, the wavefronts are moving with identical speeds since $d\rho = 1$. Since this speed is within 2% of $c_{min} = 2$, this speed is acceptable. The terms $U(0)$ and $V(0)$ represent the initiation of the wave, with

the initial conditions of $U(0) = 0.3$, $V(0) = 0.5$ true at the first five grid points, everywhere else they are zeroes, the unstable trivial states. The code was designed to plot the travelling wavefront at every $j_0 = 2000$ time steps. Since there are 6 wavefronts present in figure 6, these are at time steps $2000, 4000, 6000, 8000, 10000$ and 12000. By multiplying these values by the time step size, $ht = 0.004$, we are able to calculate the corresponding times of each wavefront in figure 6: 8, 16, 24, 32, 40 and 48.

As expected, the wavespeeds do not change for varying values of b_1 and b_2, when $b_1, b_2 < 1$, with the speed being maintained at 1.99. The system was tested first with $b_1 = 0.5$ and values of b_2 from 0.1 to 0.9, in increments of 0.1. This was then repeated with $b_2 = 0.5$ and altering the b_1 values. Since the c values of each calculation had a discrepancy of $< 1\%$, the wavespeed can be classed as constant. Since $b_1, b_2 < 1$, the wavespeed requirements from the analytic calculations of $c_{min} = 2\sqrt{1 - b_1}$ and $c_{min} = 2\sqrt{d(1 - b_2)}$ are both less than $2\sqrt{d\rho}$. Therefore, the minimum required speed is based on $2\sqrt{d\rho}$, meaning there is no dependency on b_1 and b_2, with the numerical results confirming this statement.

The initial concentrations of u and v were also found to have no effect on the resultant c. For the same values of d, b_1 and b_2 as seen in figure 6, different initial conditions were tested to ensure wavespeed was maintained. The tested values, along with their respective wavespeed were:

$$u = 0.1, v = 0.5 \Rightarrow c = 1.9936$$

$$u = 0.5, v = 0.2 \Rightarrow c = 1.9903$$

$$u = 0.8, v = 0.5 \Rightarrow c = 1.9903$$

As stated in analytics, the wavefront transitions from the unstable steady state $(0, 0)$ to the stable coexistence state. This was expected since for values of $b_1, b_2 < 1$, there exists only one stable point at which the coexistence of the competing species is possible, with all trajectories tending to this point. Despite a lower initial population, the higher equilibrium state of u is a result of its greater competitive effect on species v, than the opposing effect of v on u.

Since the wavefronts involve transitions from the steady state $(0, 0)$, equation (34) indicates that the wavespeed c should follow $c_{min} = 2\sqrt{d\rho}$. Therefore, we can use MATLAB to test the effects of varying the values of d and ρ on the resultant wavespeed in this case. There are two cases to consider when testing the dependence on d and ρ:

- Wavefronts move with different speed
- Wavefronts move with equal speeds

Therefore, the system will be tested in different ways to determine the dependency on d and ρ. It can be observed that changing d when ρ remains constant, or changing ρ when d remains constant, creates identical results.

6.1.1 Wavefronts moving with different speeds

In both of these cases, the wave profiles of each species will move with different speeds. Over time, this creates an increasing separation between the wavefronts which results in the wave profiles transitioning between different steady states. Therefore, the MATLAB code is adjusted to create the ability to test the system for these two cases and understand what happens. The medium size and total time are increased to 400 to allow the wavefront speeds to saturate and ensure they aren't affected by the boundary.

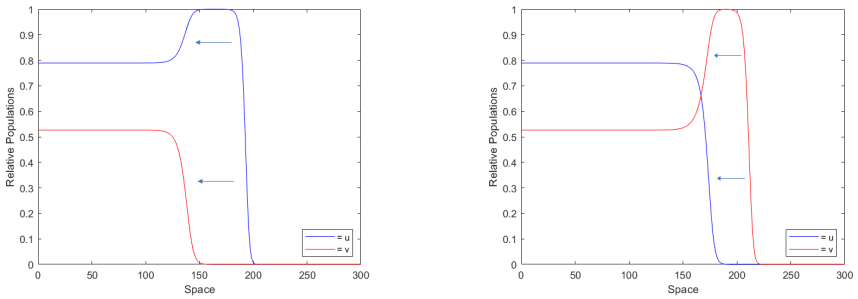

(a) $d = 0.8, \rho = 1, c = 1.9903$ (b) $d = 1.2, \rho = 1, c = 1.7516$

Figure 7: **Wave profiles with multiple transitions.** Wave profiles for the two cases in which the wavefronts move with different speeds, when $b_1 = 0.4, b_2 = 0.6$. The initial conditions are identical to those seen in figure 6 and the wave profiles of both figures are plotted at time 99.

Figures 7 (a) and (b) show the transitions between different steady states when $d\rho < 1$ and $d\rho > 1$. The code was manipulated to only produce one wave for each species, to provide a clearer view of the transitions between different states. In (a), a diffusion coefficient less than 1 means the wave profile of v moves slower than that of u, with v transitioning from $(1, 0)$ to the coexistence equilibrium, while u transitions from $(0, 0) \to (1, 0) \to$ coexistence. These new transitions in turn alter the minimum required wavespeed. The wavefronts of v now follow $c_{min} > 2\sqrt{d\rho(1 - b_2)}$ due to moving from the state $(1, 0)$. The wavefronts for u here move with constant speed 2 since they involve transitioning from $(0, 0)$. In (b), $d\rho > 1$ means the wavefronts of v are moving faster than those of species u, with v transitioning from $(0, 0) \to (0, 1) \to$ coexistence and u moving from $(0, 1)$ to coexistence. The transition from $(0, 0)$ for species v means it follows the minimum speed requirement $c_{min} > 2\sqrt{d\rho}$. Since the wavefronts of u move from the steady

state $(0, 1)$, equation (36) shows that the minimum speed requirement is $c_{min} = 2\sqrt{1 - b_1}$, meaning it is independent of d and ρ.

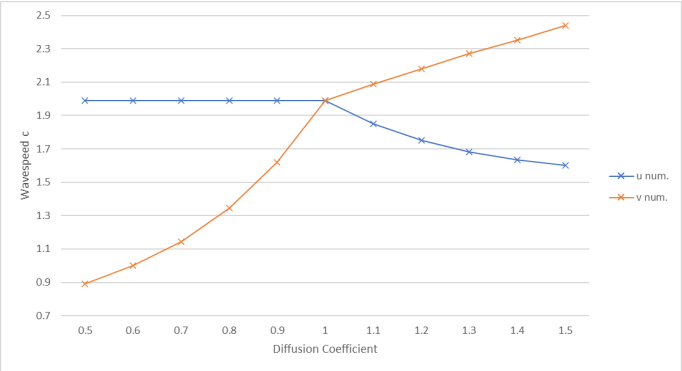

Figure 8: **Numerical wavespeeds of figure 7.** The lines show how the numerical wavespeed changes for varying diffusion coefficients d, when $\rho = 1$.

Figure 8 shows the numerical results of figure 7 for different diffusion coefficients d, provided ρ remains constant. When $d = 1$ and ρ is changed from $0.5 \rightarrow 1.5$, the numerical wavespeed calculations for u and v are the same as the results seen above, as expected.

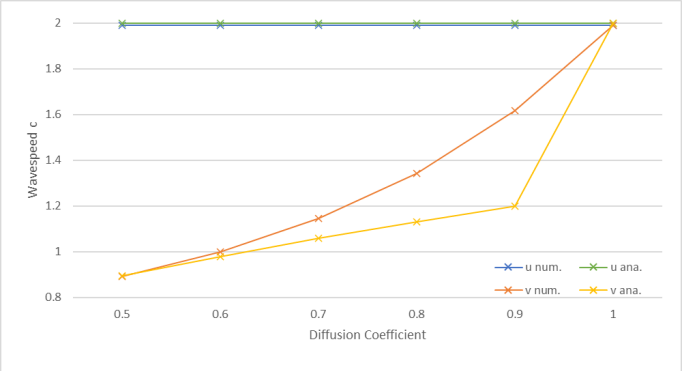

Figure 9: **Analytic vs numerical wavespeeds when v < u, relating to figure 7.** The wavefronts of v are moving slower than those of u. The analytic results stem from $c_{min} = 2$ and $c_{min} = 2\sqrt{d\rho(1 - b_2)}$ for u and v respectively.

Figure 9 shows how the numerical wavespeeds for each species compare to the analytic results, when $d\rho \leq 1$. The calculated wavefront speeds for species u confirm the analytic results of $c_{min} = 2$ for all d. This highlights that the wavefront speeds of u are constant when u is moving faster than species v. However, it can be observed that there are discrepencies between the analytic and numerical results for species v. While this is

unexpected, the numerical results do converge to the analytic minimum $c_{min} = 2\sqrt{d\rho(1-b_2)}$ as d decreases. As explained in section 3, wave profiles with exponential form result in wavespeeds that decay over time rather than appear as step functions. Since the wave profiles for v in figure 7 decay exponentially, this explains the convergence to the analytic results rather than matching them exactly. Despite this, the analytic results only provide a minimum speed requirement, therefore the numerical results can be classed as viable as they are above the analytic requirements.

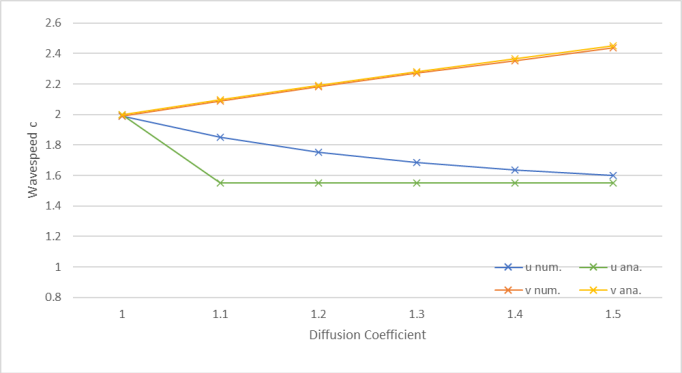

Figure 10: **Analytic vs numerical wavespeeds when v > u, relating to figure 7.** The wavefronts of v are moving faster than those of species u. The analytic results stem from $c_{min} = 2\sqrt{1-b_1}$ and $c_{min} = 2\sqrt{d\rho}$ for u and v respectively.

Figure 10 shows the comparison between the analytic and numerical results when $d\rho \geq 1$. From this figure we can draw two conclusions. Similarly to figure 9, there is convergence between the analytic and numerical results for the slower wavefronts, in this case relating to species u, due to the shape of the wave profiles. Again, since the analytic results provide a minimum wavespeed requirement, the numerical results can be classed as viable since they are not below the threshold of $c_{min} = 2\sqrt{1-b_1}$. It is also found that the wavefronts for species v move with speed $c = 2\sqrt{d\rho}$, provided they are moving faster than the profiles of species u. This is in contrast to species u moving with constant speed when the speed of u is greater than species v. To test if this fact also holds for $d\rho < 1$, we must make a slight modification to system (26):

$$\begin{cases} u_t = 0.5u_{xx} + u(1-u-b_1v) \\ v_t = dv_{xx} + \rho v(1-v-b_2u) \end{cases} \tag{44}$$

By using a diffusive constant of 0.5 for species u, we ensure that the wave profiles are always moving slower than those of species v, for all values of d from 0.5 to 1.5.

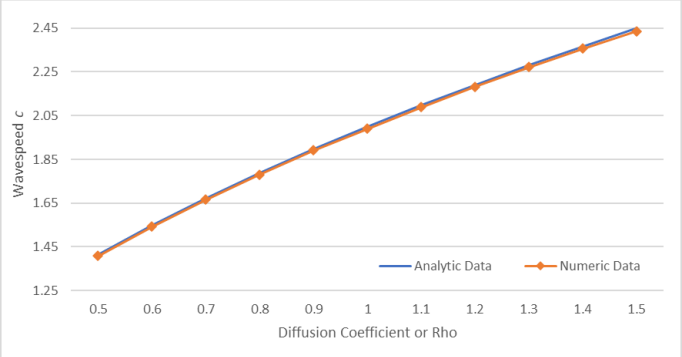

Figure 11: **Wavespeeds of v in system 44.** Line showing how the wavespeed of species v changes for different diffusion coefficients d based on our analytic and MATLAB results, subject to the conditions seen in figure 6 and when the wavefronts of v are always moving faster than those of u. The analytic results stem from $c_{min} = 2\sqrt{d\rho}$.

Figure 11 confirms that the numerical wavespeeds for species v follow the analytic results of $c_{min} = 2\sqrt{d\rho}$ for varying values of d when $\rho = 1$. The results would be identical for varying ρ provided $d = 1$.

Despite being slightly below the minimum required wavespeed based on the analytic caluclations, the results follow the same general trend and since the results are within an error margin of 2%, they are regarded as accurate. There is always a minor discrepancy between analytic and numerical results, stemming from the numeric calculations being approximations. Using smaller space steps in the MATLAB calculations would make the scheme more accurate, however while the results will incrementally approach $c = 2\sqrt{d\rho}$, they generally never reach it. The calculated wavespeeds are as follows:

Diffusion	Analytic	Numerical
0.5	1.4142	1.4078
0.6	1.5492	1.5416
0.7	1.6733	1.6661
0.8	1.7889	1.7809
0.9	1.8974	1.8915
1.0	2	1.9903
1.1	2.0976	2.0890
1.2	2.1909	2.1815
1.3	2.2804	2.2714
1.4	2.3664	2.3569
1.5	2.4495	2.4364

Table 1: The relative wavespeed for each diffusion coefficient from 0.5 to 1.5, based on analytic minimum $c_{min} = 2\sqrt{d\rho}$ and numerical results.

6.2 Transitions from trivial unstable steady state to monoculture states

The previous figures have involved a system in which the competition coefficients b_1, b_2 are less than one. We will now determine the effect on the results of either one or both coefficients being greater than one.

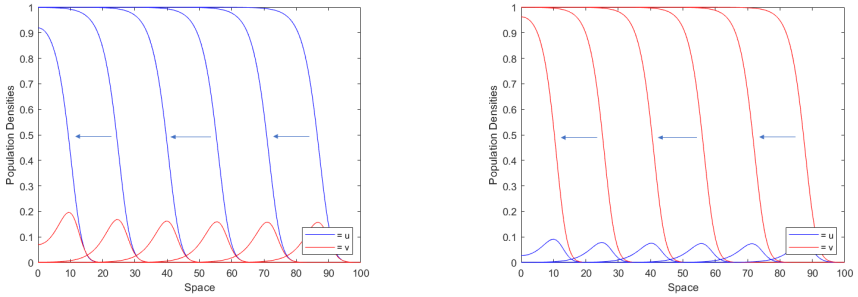

(a) $b_1 = 0.4$, $b_2 = 1.6$ (b) $b_1 = 1.6$, $b_2 = 0.4$

Figure 12: **Transitions from (0,0) to (1,0) and (0,1) case 1.** Wave profiles over time for two cases of varying competition coefficients, $b_1 < 1, b_2 > 1$ and $b_1 > 1, b_2 < 1$. $d = \rho = 1$ and $U(0) = 0.3$, $V(0) = 0.5$ are true for the first 5 grid points, elsewhere they are zeroes. The wave profiles are plotted at times 8, 16, 24, 32, 40 and 48.

Figure 12 (a) shows the wavefront transitioning from the steady state $(0, 0)$ to $(1, 0)$. Figure 12 (b) shows the wavefronts moving between the steady states $(0, 0)$ and $(0, 1)$. This is expected, due to the fact that in

the case $b_1 < 1, b_2 > 1$, there exists only one stable point $(1, 0)$ with all trajectories tending towards this point, while for $b_1 > 1, b_2 < 1$, the only existing stable point is $(0, 1)$. The wavespeeds are calculated as c=1.9903 in both (a) and (b), with (a) referring to the speed of u and (b) referring to the speed of v. Since c is the same for both u and v, there is no detriment to the results when using the code to measure for the different populations. Again, the calculated speed is within 2% of $c_{min} = 2$, so it is deemed to be acceptable.

Again, the MATLAB results prove that b_1, b_2 and the initial conditions have no affect on the wavespeed. In (a), $b_2 > 1$ means the wavespeed condition of $c_{min} > 2\sqrt{d\rho(1 - b_2)}$ becomes imaginary. Therefore, this condition can be ignored since complex numbers are not ordered in the same way as real numbers, meaning they cannot be similarly compared. This means the minimum wavespeed required is maintained at $2\sqrt{d\rho}$, meaning the numeric results validate the analytic results. Similarly in (b), the condition $c_{min} > 2\sqrt{1 - b_1}$ becomes imaginary since $b_1 > 1$, meaning the minimum wavespeed required is maintained at $2\sqrt{d\rho}$. Therefore, since the wavespeeds are only affected by the diffusion coefficient, the resultant speeds are the same as seen in figure 11, hence plots of numeric data versus analytic data are not required to avoid repetition.

The following figures will explore the outcomes of the system when $b_1, b_2 > 1$. For this case, the resultant state of the system is depdendent on two factors: the competition coefficients b_1 and b_2, as well as the initial conditions $U(0)$ and $V(0)$.

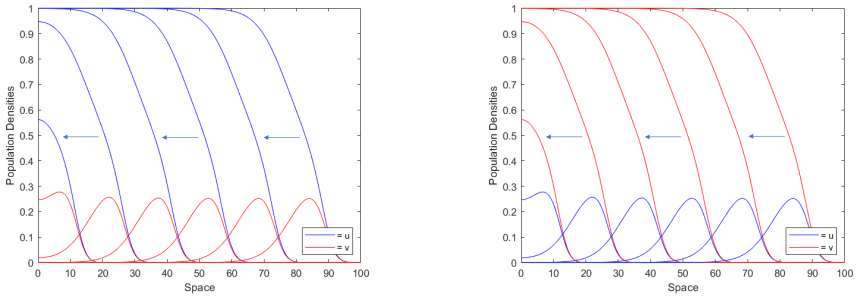

(a) $b_1 = 1.4$, $b_2 = 1.6$ (b) $b_1 = 1.6$, $b_2 = 1.4$

Figure 13: **Transitions from (0,0) to (1,0) and (0,1) case 2.** Wave profiles over time for the case when, $b_1, b_2 > 1$. In (a), $b_1 < b_2$. In (b), $b_1 > b_2$. $d = \rho = 1$, $U(0) = 0.5$, $V(0) = 0.5$ for the first 5 grid points with zeroes elsewhere. The wave profiles are plotted at times 8, 16, 24, 32, 40 and 48.

Figures 13 (a) and (b) highlight how the system is affected by the values of the competitive factors b_1 and b_2, when the initial populations of u and

v are equal. Figure (a) shows the wavefronts transitioning from $(0,0)$ to $(1,0)$. Since the competitive effect of u on v, b_2 is greater than the opposing effect of v on u, b_1, species u reaches its maximum carrying capacity. Figure (b) highlights the opposite case, when the competitve effect of v on u is greater than the effect of u on v. Here, the wavefronts move from $(0,0)$ to the steady state $(0,1)$. In both cases, the wavefronts are always moving with speed $c = 1.9903$, which confirms the analytic results of $c_{min} = 2$.

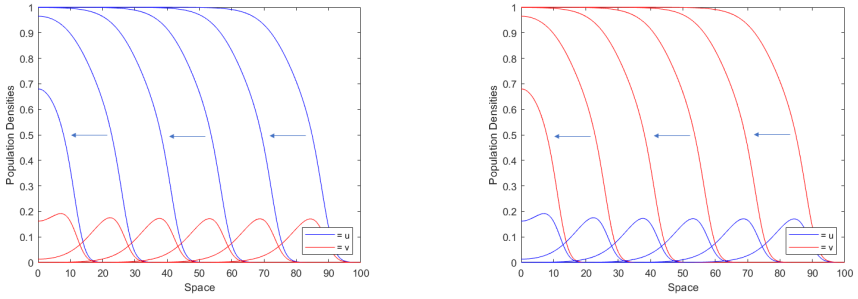

(a) $U(0) = 0.5$, $V(0) = 0.3$ (b) $U(0) = 0.3$, $V(0) = 0.5$

Figure 14: **Transitions from (0,0) to (1,0) and (0,1) case 3.** Wave profiles over time for the cases when, $b_1, b_2 > 1$. In (a), $U(0) > V(0)$. In (b), $U(0) < V(0)$, with the initial conditions true for the first five grid points. $d = \rho = 1$, $b_1, b_2 = 1.5$. The wave profiles are plotted at times 8, 16, 24, 32, 40 and 48.

As mentioned, the initial conditions also impact the outcome of the system. When $b_1 = b_2$, the species with the greater initial population density will dominate, as shown in figures 14 (a) and (b). Again, (a) involves the wavefronts moving from $(1,0)$ to $(0,0)$, while the wavefronts in (b) move from $(0,1)$ to $(0,0)$. The wavefronts move with speed $c = 1.9903$. Transitions to these respective steady states were expected, as for values of $b_1, b_2 > 1$ there exist two stable points $(1,0)$ and $(0,1)$, with a separatrix passing through that splits their domains of attraction. This means the resultant steady state that is achieved is dependent on the domain in which the initial conditions lie in, with $u > v$ tending to $(1,0)$, while $v > u$ tends to $(0,1)$.

As expected, all the numerical wavespeed results involving wavefronts transitioning from the unstable steady state $(0,0)$ were found to have no dependency on b_1 or b_2. This expectation stems from the analytic calculation of minimum wavespeed $c_{min} > 2\sqrt{d\rho}$ seen in equation (34), where c_{min} only depends on d and ρ.

6.3 Transitions from unstable steady states (1,0) & (0,1)

So far, we have only explored cases which involve the wavefronts transitioning from the steady state $(0, 0)$. However, it is possible for the wavefronts to move between two other equilibria. In these examples, the corresponding minimum wavespeed will be different to the wavefronts involving transitions from $(0, 0)$. Here, the minimum requirement will be based $c_{min} = 2\sqrt{d\rho(1 - b_2)}$ and $c_{min} = 2\sqrt{1 - b_1}$, as stated in the analytic results section.

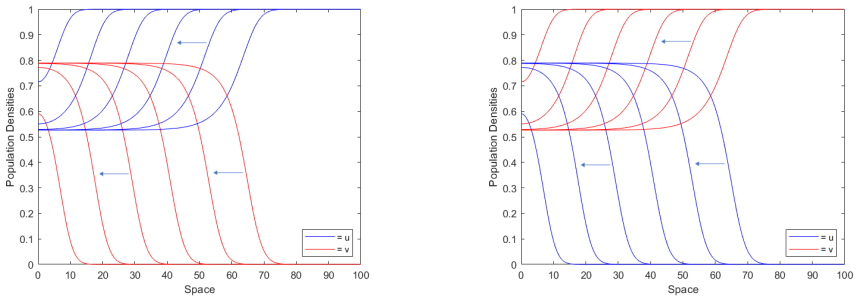

(a) $b_1 = 0.6, b_2 = 0.4$ (b) $b_1 = 0.4, b_2 = 0.6$

Figure 15: **Transitions from (1,0) and (0,1) to coexistence.** $d = \rho = 1, U(0) = V(0) = 0.5$ in the first five grid points, everywhere else they are $(1, 0)$ in (a), but $(0, 1)$ in (b). The wave profiles are plotted at times 8, 16, 24, 32, 40 and 48.

Figures 15 (a) and (b) show the evolution of a system in which the wavefronts are moving between different steady states, when $b_1, b_2 < 1$. Since $b_1, b_2 < 1$, one of the steady states involved will be the stable coexistence state. In (a), the wavefronts transition between the coexistence equilibrium and $(1, 0)$, while in (b), they move between the coexistence equilibrium and $(0, 1)$. As expected, the wavespeed c is the same for both systems, with $c = 1.4668$.

However, the wavespeed is found to be affected by the relative values of b_1 and b_2. For case (a), the wavespeed is unaffected when b_1 varies and b_2 remains constant. For case (b), the wavespeed was found to be unaffected when b_1 remains constant and b_2 is changing. By using the MATLAB code when $b_1 = 0.6$ and changing b_2 from 0.1 to 0.9 in increments of 0.1, the wavespeeds for case (b) were found to be:

b_1	b_2	Analytic	Numerical
0.1	0.6	1.8974	1.8858
0.2	0.6	1.7889	1.7721
0.3	0.6	1.6733	1.6610
0.4	0.6	1.5492	1.5363
0.5	0.6	1.4142	1.3993
0.6	0.6	1.2649	1.2470
0.7	0.6	1.0954	1.0717
0.8	0.6	0.8944	0.8712
0.9	0.6	0.6325	0.5922

Table 2: The wavespeed calculations for figure 15 (b), when b_2=0.6 and b_1 varies. The speeds are based on the analytic minimum $c_{min} = 2\sqrt{1-b_1}$, along with the MATLAB results.

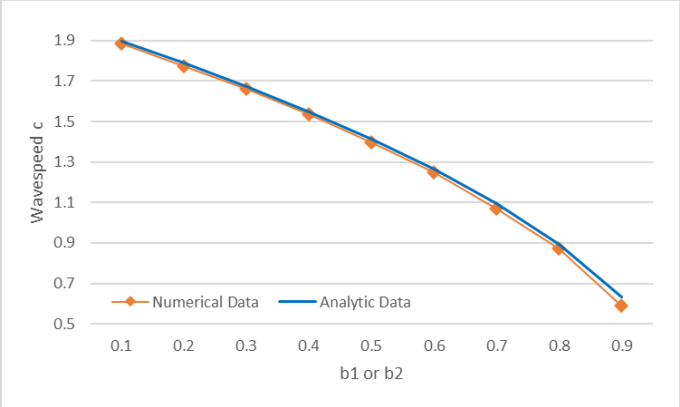

Figure 16: **Analytic vs numerical wavespeeds for figure 15.** $b_1, b_2 < 1$. Since the numerical results are identical when either b_1 or b_2 are changing, along with identical analytic results, as $d = \rho = 1$, figure 16 applies to both figures 15 (a) and (b).

These results are identical to the wavespeeds obtained for case 15 (a), when $b_1 = 0.6$ and b_2 is changed from $0.1 \rightarrow 0.9$. Therefore, figure 15 (a) has a dependency on b_2, while 15 (b) has a dependency on b_1. From equations (35) and (36), we can see this is expected since the eigenvalues for $(1, 0)$ depend on b_2, while for $(0, 1)$ the eigenvalues depend on b_1. We can conclude the numerical results are consistent with the analytic calculations.

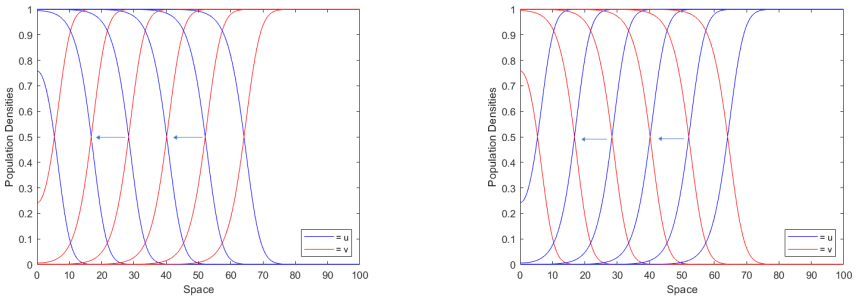

(a) $b_1 = 0.4, b_2 = 1.6$ (b) $b_1 = 1.6, b_2 = 0.4$

Figure 17: **Transitions between states (1,0) and (0,1).** $d = \rho = 1, U(0) = V(0) = 0.5$ in the first five grid points. The wavefronts move right to left, from $(0,1) \to (1,0)$ in (a) and from $(1,0) \to (0,1)$ in (b). The wave profiles are plotted at times 8, 16, 24, 32, 40 and 48.

Figures 17 (a) and (b) show the evolution of the system when either $b_1 < 1, b_2 > 1$ or $b_1 > 1, b_2 < 1$, again with the wavefronts moving between different steady states. This time however, the wavefronts are transitioning from $(0,1)$ to $(1,0)$ in (a) and from $(1,0)$ to $(0,1)$ in (b). In these cases, it is found that $c = 1.4716$. Similar to before, the MATLAB code was used to investigate the effect of b_1 and b_2 on c. From our analytic minimum wavespeed calculations for the points $(1,0)$ and $(0,1)$, we again expect to find dependencies on b_2 and b_1 respectively. However, since either $b_1 > 1$ or $b_2 > 1$, either equation (35) or (36) will become imaginary. As previously stated, imaginary wavespeed requirements can be excluded.

It is found that the wavespeed in case 17 (a) is unaffected when $b_1 = 0.4$ and the value of b_2 varies from $1.1 \to 1.9$. The opposite is also true for case 17 (b). For case (a), the corresponding wavespeeds for varying b_1 values are:

b_1	b_2	Analytic	Numerical
0.1	1.6	1.8974	1.8902
0.2	1.6	1.7889	1.7819
0.3	1.6	1.6733	1.6661
0.4	1.6	1.5492	1.5421
0.5	1.6	1.4142	1.4054
0.6	1.6	1.2649	1.2558
0.7	1.6	1.0954	1.0854
0.8	1.6	0.8944	0.8841
0.9	1.6	0.6325	0.6643

Table 3: The wavespeed calculations for figure 17 (a), based on the analytic minimum $c_{min} = 2\sqrt{1 - b_1}$, along with the MATLAB results.

These results are identical to the speeds calculated for figure 17 (b), but in this case b_1 is constant while b_2 varies. The analytic speeds for (b) in this case would stem from $c_{min} = 2\sqrt{d\rho(1-b_2)}$, where $d = \rho = 1$. Therefore, it can be deduced that figure 17 (a) is dependent on b_1, while figure (b) is dependent on b_2. This confirms the analytic results, since figure 17 (a) transitions from the steady state $(0, 1)$, which has the minimum speed requirement $c > c_{min} = 2\sqrt{1-b_1}$, whereas figure (b) transitions from $(1, 0)$, which involves the minimum $c > c_{min} = 2\sqrt{d\rho(1-b_2)}$.

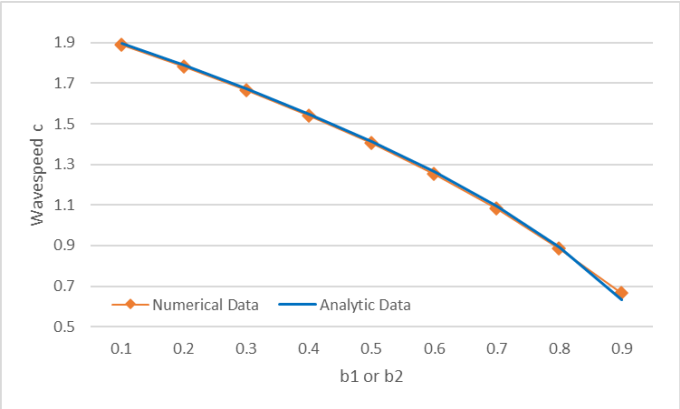

Figure 18: **Analytic vs numerical wavespeeds for figure 17 (a).** $b_2 = 1.6$, b_1 varies. The results correspond to those seen in table 3. The analytic results come from $c = 2\sqrt{1-b_1}$.

The numerical results in figure 18 are found to be identical for the wavespeeds relating to figure 17 (b) when $b_1 = 1.6, b_2 = 0.4$. This is expected since $d = \rho = 1$, meaning the minimum wavespeed requirements of $c_{min} = 2\sqrt{1-b_1}$ and $c_{min} = 2\sqrt{d\rho(1-b_2)}$ are identical when $b_1 = b_2 = 0.4$.

6.4 Transitions between stable steady states (1,0) & (0,1)

In the cases when $b_1, b_2 > 1$, the states $(1, 0)$ and $(0, 1)$ are stable, while the other two states $(0, 0)$ and coexistence are unstable. Subject to these conditions, wavefront transitions are possible from any of the four states to either of the stable states $(1, 0)$ or $(0, 1)$. Since transitions from the unstable $(0, 0)$ when $b_1, b_2 > 1$ have already been discussed in figures 13 and 14, this section will focus on transitions in a multistable system between the steady states $(1, 0)$ and $(0, 1)$.

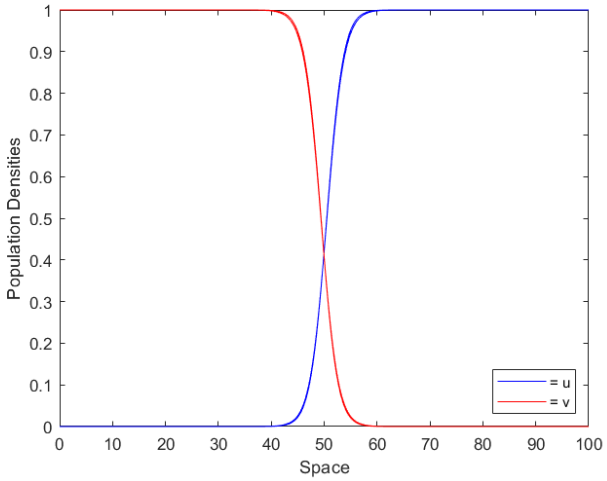

Figure 19: **Stationary profiles between steady states.** $d = \rho = 1$, $b_1 = b_2 = 1.5$. The initial conditions of the system are split between the steady states $(0, 1)$ and $(1, 0)$ on the left and right respectively.

The wavespeed for this system is found to be $c = 0$. Since $b_1, b_2 > 1$, the system is multistable containing two stable steady states $(1, 0)$ and $(0, 1)$, with the systems' parameters determining the resultant equilibrium. In figure 19, $b_1 = b_2 = 1.5$, meaning there is symmetry and the system stabilises between the two steady states, resulting in inert wavefronts. Therefore, the calculated wavespeed $c = 0$ was expected and there are no travelling wavefront solutions to be found. The wave profiles in figure 19 are plotted at time 10. Up to this time the waves are slightly moving, before the system freezes at equilibrium and the wavefronts become stationary. This is known as a transient solution. If the profiles were stationary from time 0, step functions would appear as opposed to the sloping wavefronts seen.

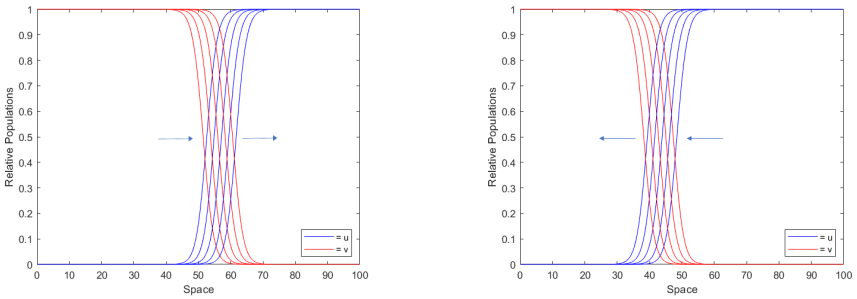

(a) $b_1 = 1.6, b_2 = 1.4$ (b) $b_1 = 1.4, b_2 = 1.6$

Figure 20: **Transitions between steady states (1,0) and (0,1).** $d = \rho = 1$. (a) moves from left to right from $(0,1) \to (1,0)$ with speed $c = 0.1138$. (b) moves right to left from $(1,0) \to (0,1)$ with speed $c = -0.1138$. The initial conditions for the system are $(0,1)$ in the left half of the medium and $(1,0)$ in the right half. The wave profiles are plotted at times $20, 40, 60, 80$ and 100.

In figures 20 (a) and (b), $b_1, b_2 > 1$ but $b_1 \neq b_2$, meaning travelling wavefront solutions exist since the wavefronts are no longer stationary. However, the two contrasting cases highlight how in the case of $b_1 > b_2$, the wavefronts are moving from left to right with positive speed, while in the case of $b_1 < b_2$, the wavefronts move left with negative speed. In figure 19, the competition coefficients are equal meaning the system stabilises in the centre. However in this case, the species with the greater competitve effect will dominate, causing the movement of the wavefronts.

b_1	b_2	Wavespeed
1.9	1.1	0.4738
1.9	1.2	0.3825
1.9	1.3	0.3063
1.9	1.4	0.2400
1.9	1.5	0.1800
1.9	1.6	0.1288
1.9	1.7	0.0813
1.9	1.8	0.0388
1.9	1.9	0

Table 4: The wavespeed calculations subject to the parameters $b_1, b_2 > 1$, $b_1 \geq b_2$, when b_1 remains constant and b_2 varies. The wavefronts are moving left to right from $(0,1)$ to $(1,0)$.

The above table provides the resultant wavespeeds when $b_1 \geq b_2$ and

highlights how in this case, the wavefronts are moving from left to right with positive speed. It is also clear that the wavefronts move with greater speed when there is a larger discrepency between the competition coefficients, as well as reaffirming that $c = 0$ when $b_1 = b_2$.

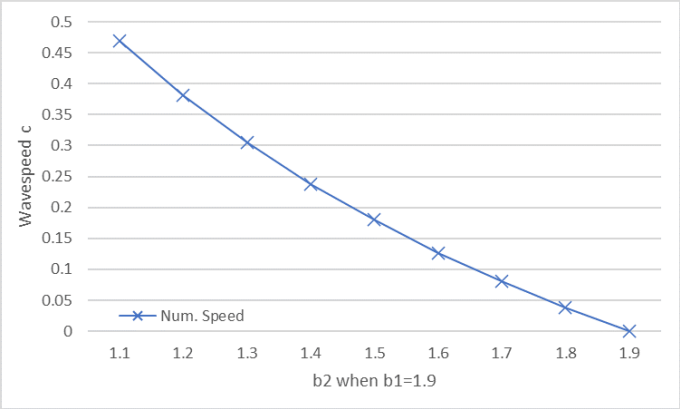

Figure 21: **Plot of numerical wavespeeds seen in table 4.** Line showing the change in wavespeed when $b_1 = 1.9$ and b_2 varies, provided $b_2 > 1$.

b_1	b_2	Wavespeed
1.1	1.1	0
1.1	1.2	-0.1188
1.1	1.3	-0.2038
1.1	1.4	-0.2688
1.1	1.5	-0.3225
1.1	1.6	-0.3675
1.1	1.7	-0.4063
1.1	1.8	-0.4413
1.1	1.9	-0.4763

Table 5: The wavespeed calculations subject to the parameters $b_1, b_2 > 1$, $b_1 < b_2$, when b_1 remains constant and b_2 varies. The wavefronts are moving right to left from $(1, 0)$ to $(0, 1)$.

The table above highlights the contrasting case when $b_1 < b_2$, showing how the wavefronts move with negative speed due to transitioning from right to left.

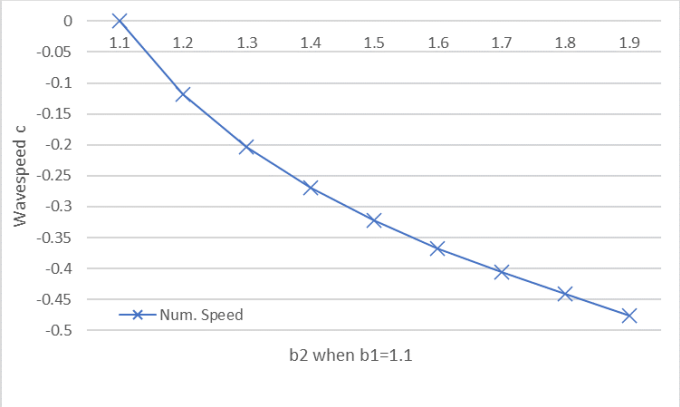

Figure 22: **Plot of numerical wavespeeds seen in table 5.** Line showing the change in wavespeed when $b_1 = 1.1$ and b_2 varies, provided $b_2 > 1$.

As expected, the wavespeeds follow the same trend as the case when $b_1 > b_2$, with the modulus wavespeeds of $b_1 = 1.9, b_2 = 1.1$ and $b_1 = 1.1, b_2 = 1.9$ being near enough identical.

While numerical simulations are possible and allow us to understand the behaviour of the resultant travelling wavefronts in a system where $b_1, b_2 > 1$, finding analytic solutions has proven to be very complex. Papers by Kan-On [5] and Girardin [4] have explored this topic to try and determine the analytics of this case, but so far no exact solutions have been found. However, Kan-On was successful in determining certain conditions applicable to the results.

For a family $(u, v)(\mathcal{E}; \rho, b_1, b_2)$ with $s(\rho, b_1, b_2)$, where $s(\rho, b_1, b_2)$ represents the wavespeeds dependent on the three variables ρ, b_1 and b_2:

- $s(\rho, b_1, b_2)$ satisfies $-2 < s(\rho, b_1, b_2) < 2\sqrt{d\rho}$, implying there is a defined range in which the wavespeeds must fall
- $\frac{\partial}{\partial \rho} s(\rho, b_1, b_2) > 0$, $\frac{\partial}{\partial b_1} s(\rho, b_1, b_2) < 0$, $\frac{\partial}{\partial b_2} s(\rho, b_1, b_2) > 0$
- Each wavespeed is unique

While there are unfortunately no analytic solutions to use as a basis for comparison for the numerical results seen in tables 4 and 5, the results are consistent with the determined range of $-2 < s(\rho, b_1, b_2) < 2\sqrt{d\rho}$.

7 Discussion

Since travelling waves are a fundamental part of many mathematical areas, especially in reaction-diffusion systems, the study of travellling wave theory has been an area of growing interest. The recent advancements in technology and computational methods has had a significant impact on their use in mathematical models which have a wide range of applications. Being most fully developed for systems of partial differential equations, travelling wave solutions are of growing importance in mathematical modelling. One reason for this is the fact that analytic results are often not possible to determine. Therefore, numerical simulations allow us to understand the behaviour of a system as it evolves over time.

In the beginning of this paper, the theory of travelling waves was detailed, followed by the introduction of the Fisher equation as an example of how to generate travelling wave solutions. This gave us a base understanding of the process of deriving these results, including how to determine the minimum wavespeed requirement for the system and what this means. We then moved onto another form of reaction diffusion equation, the Fitzhugh equation. In the same way as with the Fisher equation, travelling wavefront solutions were derived, however in this case the wavespeed was found to be unique as opposed to simply a minimum requirement. A second method of solving this equation, as a product of integral terms, was also briefly described.

Moving forward, the analytic study of the Lotka-Volterra competition model was explored, with the process of nondimensionalisation utilised to create a dimensionless system for later use. Through substitution of the travelling wave solution form into this system, we were able to derive a system of first order ODEs from the original second order system. This allowed us to use MATLAB to construct the 4x4 Jacobian matrix of the system and generate the respective matrix of equilibrium states, from which each corresponding set of eigenvalues was calculated. From these eigenvalues, we were able to determine minimum wavespeed requirements of each steady state, based on the condition that each eigenvalue must be real. For the point $(0, 0)$, there arose two unequal wavespeed conditions, $c_{min} = 2$ and $c_{min} = 2\sqrt{d\rho}$. While the discrepancy between the two conditions was not initially understood, it proved to become one of the more interesting findings of this paper. It was determined that the wavespeed requirements were not shared by the wavefronts of each species, with the fronts for species u adhering to one speed requirement, while the second requirement applied to the wavefronts of species v. The same scenario was found to apply to the wavespeed requirements involving transitions from the points $(1, 0)$ and $(0, 1)$, with one wavespeed requirement applying to species u, while the other applied to species v. For transitions involving the states $(1, 0)$ and $(0, 1)$,

the wavespeeds were found to be dependent on the competition coefficients b_1 and b_2, while transitions involving the state $(0, 0)$ were independent of these.

We then discussed the numerical scheme that was used in the later simulations, the explicit finite forward difference method. This method solves the differential equations through finite difference approximations of the derivatives. By converting the system into a set of recurrence relations, it was shown how approximations of the time and space derivatives were used to create successive results. Since this system can be unstable, Neumann stability analysis was applied to find the set of values for which the system was numerically stable and how this was applied in the MATLAB code.

In section 6, numerical simulations for the system were ran using MATLAB, subject to varying parameters and conditions, to understand the behaviour and evolution of the system in different cases. Beginning with transitions from the trivial unstable steady state to the coexistence equilibrium, we first explored the system when the wavefronts of each species are moving with the same speed and plotted their evolution over time. Transitions between these states occur when both $b_1, b_2 < 1$. The system was tested using varying competition coefficients and initial conditions to verify the results were independent of these factors, as per the analytics. We then ran the simulations for the case when the wavefronts of each species move with different speeds. As opposed to a single transition between steady states when moving with equal speeds, it was found here that different speeds resulted in multistage transitions of the wave profiles. Because of this, the minimum wavespeed requirements changed due to the involvement of the steady states $(1, 0)$ and $(0, 1)$, as opposed to simply transitioning from $(0, 0)$. By deriving the results for the cases when the profiles of u move faster and slower than those of species v, we discovered how the two species can adhere to different wavespeed requirements, with $c_{min} > 2$ applying to species u, while $c_{min} > 2\sqrt{d\rho}$ applies to species v. However, the wavespeed requirements $c_{min} > 2\sqrt{1 - b_1}$ and $c_{min} > 2\sqrt{d\rho(1 - b_2)}$ can apply to wavefronts for both species. To confirm that $c_{min} > 2\sqrt{d\rho}$ applies to species v, we created a modified system that kept the wavefronts of u slower than v for all d or ρ, with the results consistent with this minimum wavespeed requirement.

Next, the system was tested when the wavefronts transition from the trivial unstable steady state to one of the monoculture states $(1, 0)$ or $(0, 1)$. The first case involved $b_1 < 1, b_2 > 1$ or vice versa, while case two involved $b_1, b_2 > 1$. Again, since the system involves transitioning from the state $(0, 0)$, we expected the wavespeed results to be independent of b_1 and b_2, which was found to be true. However, when $b_1, b_2 > 1$, we also confirmed that the resultant steady state achieved by the system was dependent on the competition coefficients and the initial conditions.

We then made slight modifications to the MATLAB code to allow us to test the system when transitioning from the unstable steady states $(1,0)$ and $(0,1)$. In the first simulation we used $b_1, b_2 < 1$, meaning the system transitioned to the stable coexistence state. Since the wavefronts were transitioning now from the states $(1,0)$ and $(0,1)$, we found a wavespeed dependency on b_1 and b_2, as expected. The next set of simulations involved wavefronts transitioning between the states $(1,0)$ and $(0,1)$, when one state is stable and the other is unstable. Transitions between these states in this scenario occur when $b_1 > 1, b_2 < 1$ or vice versa. Again, the numerical results confirmed the wavespeed dependency on b_1 and b_2, as per the analytic study.

Finally, the multistable system in which wavefronts transition between the two steady states $(1,0)$ and $(0,1)$ was explored. In this system, the steady states $(0,0)$ and coexistence were unstable. Transitions between these steady states were possible when $b_1, b_2 > 1$, with the resultant equilibrium achieved is dependent on the relative values of the competition coefficients. We initially demonstrated that when $b_1 = b_2$, the system stabilises between the steady states, meaning the wavefronts are motionless and there is no existence of travelling wavefront solutions. We then moved on to show how the relative size of the competition coefficients affects the direction in which the wavefronts move. For $b_1 > b_2$, the wavefronts transition from $(0,1)$ to $(1,0)$, moving left to right with positive speed. For $b_1 < b_2$, the wavefronts transition from $(1,0)$ to $(0,1)$, moving right to left with negative speed. As expected, the wavefronts were found to move faster as the discrepancy between b_1 and b_2 increased. In contrast to the previous sections however, it has not yet been possible to determine analytic solutions for the case when $b_1, b_2 > 1$, despite numerous attempts. However, Kan-On was able to define a range in which the results should lie, with our results being consistent with his findings.

When using computer simulations to model a system, the numerical results will never exactly match the analytic calculations. Reasons for this include the numerical calculations being approximations at each space step, which will always result in slight discrepencies. Therefore, provided the numerical results are within an error margin of 2% when compared to the analytics, the results are deemed as acceptable. Throughout this paper, our MATLAB results were within this acceptable margin except for two interesting cases, seen in figures 9 and 10. Here, when v moves slower then u, the numerical results for species v converged to the analytic results as d decreased. For the case when v moves faster than u, the wavefront speeds for species u converged to the analytic minimum as d increased. While these results were not expected, they can be deemed acceptable since the analytic study simply provides a minimum wavespeed requirement and the numerical results are found to be faster than this minimum.

Through completion of this project, I have managed to enhance my current knowledge relating to systems of partial differential equations and their solutions, as well as learn valuable new skills and mathematical techniques. I have developed a sound understanding of travelling waves and how to use them as a method of solving PDEs, allowing us to better understand the dynamics of the system. I have enhanced my knowledge on deriving the steady states and resultant eigenvalues of a system, in turn bettering my understanding of stability analysis and what this means with regard to minimum wavespeed requirements. Building on this, I have acquired knowledge relating to a new numerical scheme, the finite forward difference method, along with how to implement his onto a system. This method also built on my knowledge from MATH421 of Neumann boundary conditions and their importance, as well as providing me with a basic understanding of the Neumann stability analysis method. The extensive use of MATLAB when deriving numerical results throughout this project has increased my proficiency with using this software, building on the basic skills I acquired when completing the MATH552 project. Finally, thanks to my supervisor, I have developed a better understanding of how to present my findings in a suitable and coherent way, along with how to structure and format a mathematical paper.

8 References

References

[1] Nouf S. Alghamdi. *Thesis Outline*. University of Liverpool, 2019.

[2] A.B Downey. *Physical modeling in MATLAB*. Green Tea Press, 2011.

[3] Robert A. Gardner. Existence and stability of travelling wave solutions of competition models: A degree theoretic approach. *Journal of Differential Equations*, 44(3):343–364, 1982.

[4] Léo Girardin and Grégoire Nadin. Travelling waves for diffusive and strongly competitive systems: Relative motility and invasion speed. *European Journal of Applied Mathematics*, 26(4):521–534, 2015.

[5] Yukio Kan-On. Parameter dependence of propagation speed of travelling waves for competition-diffusion equations. *SIAM Journal on Mathematical Analysis*, 26(2):340–363, 1995.

[6] Yukio Kan-On. Fisher wave fronts for the lotka-volterra competition model with diffusion. *Nonlinear Analysis: Theory, Methods and Applications*, 28(1):145–164, 1997.

[7] James D. Murray. *Mathematical Biology I. An Introduction*, volume 17. Springer New York, 2002.

[8] James. D. Murray. *Mathematical biology*. Springer-Verlag, 2nd edition, 2013.

[9] William H. Press, Saul A. Teukolsky, William T. Vetterling, and Brian P. Flannery. *NUMERICAL Recipes in C*. Cambridge University Press, 2nd edition, 1988.

[10] Aizik I. Volpert, Vitaly A. Volpert, and Vladimir A. Volpert. *Travelling wave solutions of parabolic systems*, volume 140. American Mathematical Society, 1994.

[11] Yuanxi Yue, Yazhou Han, Jicheng Tao, and Manjun Ma. The minimal wave speed to the lotka-volterra competition model. *Journal of Mathematical Analysis and Applications*, 488(2), 2020.

9 Appendix 1

The following code was used to calculate the matrix of equilibrium points seen in (29) and their respective eigenvalues.

```
syms   u w v s b1 b2 c r d

 SYS= [w==0,c*w-u*(1-u-b1*v)==0,s==0,(c*s-r*v*(1-v-b2*u))/d==0];
  vars=[u w v s];
  QQ=solve(SYS, vars);
P=[QQ.u(:) QQ.w(:) QQ.v(:) QQ.s(:)]

  A=jacobian([w,c*w-u*(1-u-b1*v),s,(c*s-r*v*(1-v-b2*u))/d],[u w v s]);
  N=sym('X',[1,4]);
    A(N) = subs(A,[u, w, v, s],N);

  J1=A(QQ.u(1),QQ.w(1), QQ.v(1), QQ.s(1));
  J2=A(QQ.u(2),QQ.w(2), QQ.v(2), QQ.s(2));
  J3=A(QQ.u(3),QQ.w(3), QQ.v(3), QQ.s(3));
  J4=A(QQ.u(4),QQ.w(4), QQ.v(4), QQ.s(4));


 e1=eig(J1)
 e2=eig(J2)
 e3=eig(J3)
 e4=eig(J4)
```

10 Appendix 2

The following code was produced to generate the numerical results of system 26 and create the previously seen figures that show the evolution of the resultant wavefronts over time. The wavespeed is calculated by taking the distance between two wavefronts at the points when the waves for species v become greater than 0.5, then dividing this value by the time that has lapsed between the waves. The systems' parameters were changed to solve the system for varying cases and conditions. By reducing the size of the medium L and the total time t_{end}, the code was refined to reduce the time taken to generate the results without impacting their accuracy. The diffusion coefficient D, the competition factors b_1 and b_2, along with the initial conditions $U1(i)$ and $V1(i)$ were simply changed to test the system for different cases. However, the wavespeed c that is calculated using this code tended to have an error margin of around $4-5\%$, a level too high for acceptability. Therefore, slight adjustments were made with additional code to reduce this error to an acceptable level of $1-2\%$. This new code accounted for a moving frame of reference when calculating the speed, rather than a stationary reference point that was used in the code seen below.

```
clear;

L=100;            % size of the medium
t_end=50;       % total time
D=1.;
hx=0.1;        % space step size
ht=0.99*hx^2/(2*D);        % time step size

nh=t_end/ht;    % number of time steps
n=L/hx+1;       % number of grid points
% center=int32(n/2)

b1=0.4;       % competition factor
b2=0.6;       % competition factor

Du=D;      % diffusion coefficient
Dv=D;      % diffusion coefficient
s1=ht*Du/hx^2;
s2=ht*Dv/hx^2;

U1=zeros(n,1);
V1=zeros(n,1);
UB=zeros(n,1);
VB=zeros(n,1);
```

```
%inital conditions:
for i=1:5 %center-2:center+2
    U1(i)=0.3;
    V1(i)=0.5;
end;
%-----------------------------------------
t=0;
figure
E=0:hx:L; % Defining space
j0=2000
for j= 1:nh
    %integration
    for i=2:n-1
        u=U1(i);
        v=V1(i);
        UB(i)=u+s1*(U1(i-1)-2*u+U1(i+1))+ht*u*(1-u-b1*v);
        VB(i)=v+s2*(V1(i-1)-2*v+V1(i+1))+ht*v*(1-v-b2*u);
    end;
    %boundary conditions
    UB(1)=UB(2); UB(n)=UB(n-1);
    VB(1)=VB(2); VB(n)=VB(n-1);
    % update
     U1=UB;
     V1=VB;
    if rem(j,j0) == 0
        plot(E(1:end),U1,'b',E(1:end),V1,'r');
        hold on
    end;
    t=t+ht;
    if j==j0
        t1=t;
        for i=2:n-1
            if V1(i)>0.5
            p1=i*hx;
            end;
        end;
    end;
 end;
 t2=t;
 for i=2:n-1
     if V1(i)>0.5
         p2=i*hx;
     end;
 end;
```

```
 speed=(p2-p1)/(t2-t1);



% plotting the profiles
% plot(E(1:end),U1,'b',E(1:end),V1,'r');
 hold off
xlabel('Space')
ylabel('Population Densities')
legend({'= u','= v'},'Location','southeast')
% Equations to quantify the success of invasions.
```